Impact of High-Temperature Effects on Shock Inclination Angle in Super- and Hypersonic Flow around Sharp Cone

K.N. Volkov[1], V.N. Emelyanov[2], A.G. Karpenko[3], S.S. Tolstoguzov[2]

[1]Kingston University, London, UK

[2]Baltic State Technical University, St. Petersburg, 190005, Russia

[3]Saint Petersburg State University, St. Petersburg, 198504, Russia

Numerical simulation of a super- and hypersonic flow of an inviscid gas around a sharp cone is performed taking into account high-temperature effects. The numerical implementation of a computational procedure designed to find stationary solutions of the gas dynamics equations describing flows around a cone with the real gas properties is carried out. The influence of physical and chemical processes on the distributions of flow quantities and the angle of inclination of the shock is discussed, and the results of numerical calculations obtained with the perfect and real gas model are compared. The computational results are compared with the data obtained for a supersonic around a wedge with a similar opening half angle.

Keywords: aerodynamics, supersonic flow, shock wave, real gas, cone flow, cone.

INTRODUCTION

Interest in studies of supersonic and hypersonic flows around bodies of rotation is due to their practical applications in aviation and rocket and space technology, associated with the calculation of the aerodynamic characteristics of aircraft.

The main feature of supersonic flow around bodies of rotation is the formation of a discontinuity near the frontal part of the body, which has the effect on the shape of an attached conical shock wave under certain conditions [1, 2]. When calculating the parameters of the flow around bodies of rotation with a curvilinear generatrix, the flow in a small vicinity of the tip with a shock wave

attached to it is replaced by a conical one even at angles of attack that are not equal to zero [3]. Asymmetric flow around a V-shaped wing with supersonic leading edges and swirling conical flows are discussed in [4, 5]. The hypersonic flow around sharp bodies is investigated within the framework of the viscous-inviscid interaction model or the model of a thin shock layer. In particular, the hypersonic flow of a viscous gas in a shock layer near a sharp cone is considered in [6] based on the model of a viscous shock layer.

Conical flowfields are used to generate the bearing surfaces of waves [7]. They make it possible to obtain a higher aerodynamic quality than when using flows behind flat shock waves. The use of cones as body-generators of shock waves also makes it possible to provide a slightly larger volume intended for the payload [8]. The studies [9, 10] compare the layouts of wave-boats built on the basis of axisymmetric conical flows and flows behind two-dimensional plane shock waves.

Finding stationary solutions to the equations of gas dynamics describing the flow of a van der Waals gas around a circular cone is discussed in [11, 12]. The calculation results correspond to the case when the substance in the incoming flow is not only in a liquid or gaseous state, but also in a two-phase state. Shock-wave flows of a gas suspension are considered in [13].

The influence of physical and chemical processes on the structure of the flow between the detached shock wave and the surface of the cone is considered in [14]. In equilibrium chemical reactions, there is a strong change in the thermodynamic state of the gas mixture in the shock layer. Numerical simulation of gas-dynamic and physical and chemical processes accompanying hypersonic flow around bodies of various shapes are discussed in [15, 16]. High-temperature air models are implemented in the Russian package of computational gas dynamics and heat transfer Logos [17, 18].

Despite a fairly large number of software systems designed to solve the problems of gas dynamics and heat transfer and allowing to reduce the cost of work on the creation of new models of equipment, increasing their quality and

reliability, simpler developments used to test the performance of new models and approaches. The use of problem-oriented software systems can significantly reduce the amount of information required to describe the environment. Using gas models of varying degrees of complexity, starting with a perfect gas model and ending with a model that takes into account physicochemical processes, it allows creating optimal work programs that combine a fairly complete description of the flow with minimal computing resources and the possibility of their subsequent integration with more complex software systems.

An increase in temperature leads to the impossibility of performing calculations of flow quantities of the perfect gas model due to the ongoing chemical reactions. In this study, the conical flow approximation is applied to consider the influence of high-temperature effects in air on the supersonic and hypersonic flow around a cone with an attached shock wave. The calculation results are compared with the data obtained for a wedge with a similar opening half angle.

GOVERNING EQUATIONS

The flow is described using the equations of continuity and changes in the momentum, written in a spherical coordinate system (r, θ, φ), where r is the radial coordinate, θ is the polar anlge, φ is the circumferential angle (Figure 1). When considering a conical flow, the velocity component and derivatives in the azimuthal direction are neglected ($v_\varphi = 0, \partial/\partial\varphi = 0$).

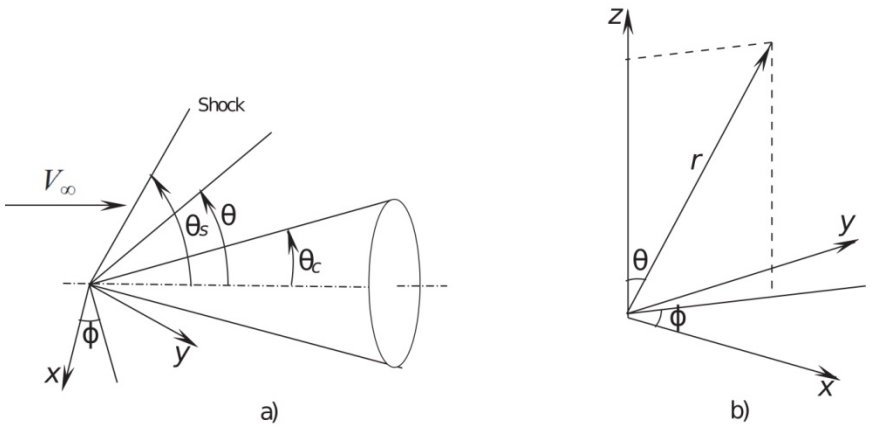

Figure 1. Flow around cone (a) and frame of reference (b)

In a spherical coordinate system, the laws of conservation of mass and momentum have the following form [1]:

– continuity equation

$$\frac{1}{r^2}\frac{\partial \rho v_r r^2}{\partial r} + \frac{1}{r\sin\theta}\frac{\partial \rho v_\theta \sin\theta}{\partial \theta} = 0;$$

– momentum equations

$$v_r \frac{\partial v_r}{\partial r} + \frac{v_\theta}{r}\frac{\partial v_r}{\partial \theta} - \frac{v_\theta^2}{r} = -\frac{1}{\rho}\frac{\partial p}{\partial r};$$

$$v_r \frac{\partial v_\theta}{\partial r} + \frac{v_\theta}{r}\frac{\partial v_\theta}{\partial \theta} + \frac{v_r v_\theta}{r} = -\frac{1}{\rho r}\frac{\partial p}{\partial \theta}.$$

Here, ρ is the density, r is the radius, θ is the polar anlge, φ is the circumferential angle, v_r and v_θ are the projections on velocity vector in spherical coordinates.

The flow incident on the cone is assumed to be uniform, and the conical shock wave has a straight generatrix. The flow behind the shock wave has isoenergetic properties, which makes it possible not to consider the differential form of the energy equation, but to replace it with the condition of constancy of the total enthalpy in the entire flow region between the shock wave and the conical surface of the cone

$$h_s + \frac{v_s^2}{2} = h + \frac{v^2}{2} = \text{const},$$

Index s denotes the quantities behind the shock.

CONICAL FLOW

When studying a supersonic and hypersonic inviscid gas flow around a cone at a zero angle of attack, the properties of conical flows are used, which make it possible to simplify the initial equations and the process of their solution. The flow around a right circular cone is axisymmetric. The flows between the surface of the

cone and the surface of the shock wave are geometrically similar in all planes perpendicular to the longitudinal axis.

A diagram of the supersonic gas flow around the cone is shown in Figure 2. The diagram also shows the angle of inclination of the shock wave to the longitudinal axis θ_s and the angle of the half opening of the cone θ_c.

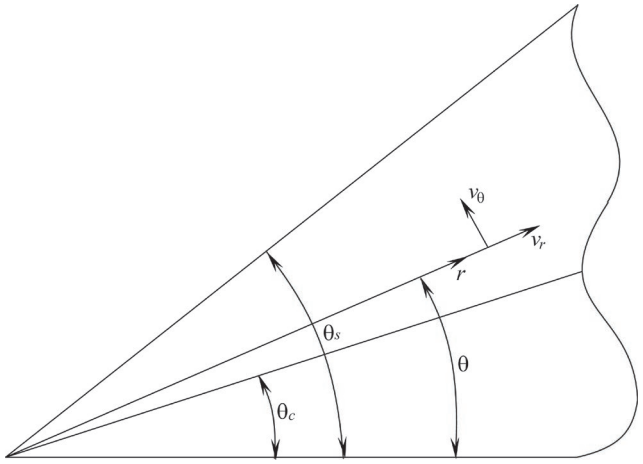

Figure 2. Supersonic flow around the cone at zero angle of attack

The governing equations are transformed under the conditions of flow conicity. In this case, the gas-dynamic and thermodynamic parameters become functions of only one independent variable which is the angle of the conical surface θ (the angle of inclination of the intermediate surface to the longitudinal axis of the cone). Euler's equations are reduced to the system of ordinary differential equations

$$2\rho v_r + v_\theta \frac{d\rho}{d\theta} + \rho \frac{dv_\theta}{d\theta} + \rho v_\theta \theta = 0;$$
$$\frac{dv_r}{d\theta} = v_\theta;$$
$$\rho v_\theta \frac{dv_\theta}{d\theta} + \rho v_r v_\theta + \frac{dp}{d\theta} = 0;$$
$$\frac{d}{d\theta}\left(h + \frac{v_\theta^2 + v_r^2}{2}\right) = 0.$$

The equation of state is added to the reduced system of equations. The boundary conditions are set on the shock surface (Rankine–Hugoniot conditions) and on the cone surface. The conditions on the discontinuity surface at $\theta=\theta_s$ have the form

$$v_r = v_{2\tau}, \quad v_\theta = -v_{2n},$$

where θ_s is the shock inclination angle, $v_{2\tau}$ is the tangential velocity behind the shock, v_{2n} is the normal velocity behind the shock. No-penetration boundary condition ($v_\theta=0$) is applied to the cone surface at $\theta=\theta_c$, where θ_c is the cone angle.

PHYSICAL AND CHEMICAL PROCESSES

In a high-temperature flow, it is necessary to take into account the real properties of the gas and their influence on the flow structure and the local behaviour of the gas-dynamic quantities. At low temperatures and pressures, the internal energy consists of the energy of the translational and rotational motion of molecules, therefore air is considered a perfect diatomic gas with a constant molecular weight, constant specific heat and a constant adiabatic index. High-temperature flows are characterized by the excitation of vibrational degrees of freedom of polyatomic molecules, the presence of dissociation and ionization processes. In air, oxygen dissociation occurs at T=2000–4000 K, and nitrogen dissociation occurs at T=4000–10000 K. At T=7000–10000 K, the ionization process begins with the formation of free electrons. At T>10000–12000 K, single ions of these components make up a significant fraction.

The internal energy of a gas consists of their energies of translational, rotational and vibrational motions of molecules, as well as of the chemical binding energy, electronic excitation and ionization. As a result of the successive excitation of atoms and molecules and the onset of the corresponding reactions, a significant part of the heat received by the air is spent on the formation of the corresponding new levels of internal energy. The temperature of a real gas, determined by the translational degrees of freedom, turns out to be less than the temperature of an ideal gas. The difference in temperatures of real and ideal gases increases with an increase in flight speed and is caused by a change in the thermodynamic properties

of a gas, determined by such parameters as specific heat capacity, adiabatic index, gas constant and molecular weight of air. In this case, the equation of state also changes, which describes the nature of the relationship between pressure, gas density and its temperature.

An advantage of the model proposed in [20] (Kraiko model, which takes into account 13 components) is that the dissociation and ionization of air at high temperatures is taken into account. When taking into account the real thermodynamic properties of air, explicit expressions are used for the density and specific internal energy in terms of pressure and temperature $\rho=\rho(p, T)$ and $\varepsilon=\varepsilon(p, T)$. In the range of temperatures from 200 to 20,000 K and pressures from 0.001 to 1000 atm, the relative error of the model does not exceed ±2%, usually falling within the band of ±1%.

The equations describing the flow of a real gas have the same form as the equations for an ideal gas. When using the Kraiko model, difficulties arise in the transition from conservative variables to physical ones. In approximate models, the state of the gas is determined as a function of the variables $\rho=\rho(p, T)$ and $\varepsilon=\varepsilon(p, T)$, and the dependence $p=p(\rho, \varepsilon)$ is used for calculations. For the transition between physical and conservative variables with known density and internal energy, a system of nonlinear equations is solved.

NUMERICAL METHOD

The two-point boundary value problem is solved using numerical integration methods. In the process of numerical integration, the polar angle changes in the range from θ_c to θ_s. Derivatives of density and enthalpy are expressed in terms of pressure and temperature

$$\frac{d\rho}{d\theta}=\frac{\partial\rho}{\partial p}\frac{dp}{d\theta}+\frac{\partial\rho}{\partial T}\frac{dT}{d\theta},\quad \frac{dh}{d\theta}=\frac{\partial h}{\partial p}\frac{dp}{d\theta}+\frac{\partial h}{\partial T}\frac{dT}{d\theta}.$$

The system of ordinary differential equations describing the flow takes the form

$$2\rho v_r + v_\theta\left(\frac{\partial\rho}{\partial p}\frac{dp}{d\theta} + \frac{\partial\rho}{\partial T}\frac{dT}{d\theta}\right) + \rho\frac{dv_\theta}{d\theta} + \rho v_\theta\theta = 0;$$
$$\frac{dv_r}{d\theta} = v_\theta;$$
$$\rho v_\theta\frac{dv_\theta}{d\theta} + \rho v_r v_\theta + \frac{dp}{d\theta} = 0;$$
$$\frac{\partial h}{\partial p}\frac{dp}{d\theta} + \frac{\partial h}{\partial T}\frac{dT}{d\theta} + v_\theta\frac{dv_\theta}{d\theta} + v_r\frac{dv_r}{d\theta} = 0.$$

In vector form, the system is

$$A\frac{dU}{d\theta} = B,$$

where

$$U = \begin{pmatrix} p \\ T \\ v_\theta \\ v_r \end{pmatrix}, \quad B = \begin{pmatrix} -\rho(2v_r + v_\theta ctg\theta) \\ v_\theta \\ -\rho v_r v_\theta \\ 0 \end{pmatrix},$$

$$A = \begin{pmatrix} v_\theta\frac{\partial\rho}{\partial p} & v_\theta\frac{\partial\rho}{\partial T} & \rho & 0 \\ 0 & 0 & 0 & 1 \\ 1 & 0 & \rho v_\theta & 0 \\ \frac{\partial h}{\partial p} & \frac{\partial h}{\partial T} & v_\theta & v_r \end{pmatrix}.$$

The inverse matrix has the form

$$A^{-1} = \frac{1}{|A|}\begin{pmatrix} A_{11} & A_{12} & A_{13} & A_{14} \\ A_{21} & A_{22} & A_{23} & A_{24} \\ A_{31} & A_{32} & A_{33} & A_{34} \\ A_{41} & A_{42} & A_{43} & A_{44} \end{pmatrix},$$

The determinant of the matrix is found from the relation

$$|A| = \rho_2 v_\theta^2\left(\frac{\partial h_2}{\partial p_2}\frac{\partial\rho_2}{\partial T_2} - \frac{\partial\rho_2}{\partial p_2}\frac{\partial h_2}{\partial T_2}\right) - v_\theta^2\frac{\partial\rho_2}{\partial T_2} + \rho\frac{\partial h_2}{\partial T_2}.$$

Here

$$A_{11} = -\rho_2 v_\theta \frac{\partial h_2}{\partial T_2}, \quad A_{12} = -\rho_2 v_r v_\theta^2 \frac{\partial \rho_2}{\partial T_2}, \quad A_{13} = -v_\theta^2 \frac{\partial \rho_2}{\partial T_2} + \rho_2 \frac{\partial h_2}{\partial T_2},$$

$$A_{14} = \rho_2 v_\theta^2 \frac{\partial \rho_2}{\partial T_2};$$

$$A_{21} = \rho_2 v_\theta \frac{\partial h_2}{\partial p_2} - v_\theta, \quad A_{22} = \rho_2 v_r \left(v_\theta^2 \frac{\partial \rho_2}{\partial p_2} - 1 \right), \quad A_{23} = v_\theta^2 \frac{\partial \rho_2}{\partial p_2} - \rho_2 \frac{\partial h_2}{\partial p_2},$$

$$A_{24} = \rho_2 \left(1 - v_\theta^2 \frac{\partial \rho_2}{\partial p_2} \right);$$

$$A_{31} = \frac{\partial h_2}{\partial T_2}, \quad A_{32} = v_\theta v_r \frac{\partial \rho_2}{\partial T_2}, \quad A_{33} = v_\theta \left(\frac{\partial \rho_2}{\partial T_2} \frac{\partial h_2}{\partial p_2} - \frac{\partial \rho_2}{\partial p_2} \frac{\partial h_2}{\partial T_2} \right),$$

$$A_{34} = -v_\theta \frac{\partial \rho_2}{\partial T_2};$$

$$A_{41} = 0, \quad A_{42} = \rho_2 \frac{\partial h_2}{\partial T_2} - \rho_2 v_\theta^2 \frac{\partial \rho_2}{\partial p_2} \frac{\partial h_2}{\partial T_2} - v_\theta \frac{\partial \rho_2}{\partial T_2} \left(v_\theta - \rho_2 v_\theta \frac{\partial h_2}{\partial p_2} \right), \quad A_{43} = 0.$$

$$A_{44} = 0.$$

For time integration, Euler method of the 1st order of accuracy is used

$$U^{n+1} = U^n + \Delta\theta A^{-1} B.$$

The physical parameters behind the shock wave (p_2, T_2, v_θ, v_r) are used as the initial conditions. The end of counting condition has the form v_θ=0.

The implementation of the algorithm for a real gas requires the calculation of the partial derivatives of enthalpy and molecular weight with respect to pressure and temperature. For a perfect gas (p=ρRT), the derivatives of density and enthalpy are found from the relations

$$\frac{\partial \rho}{\partial p} = \frac{\mu}{R_0 T}, \quad \frac{\partial \rho}{\partial T} = -\frac{p\mu}{R_0 T^2}, \quad \frac{\partial h}{\partial p} = 0, \quad \frac{\partial \rho}{\partial T} = c_p.$$

For the real gas model used, the derivatives are calculated based on the numerical differentiation formulas

$$\frac{\partial h}{\partial p} = \frac{h(p + \Delta p, T) - h(p - \Delta p, T)}{2\Delta p};$$

$$\frac{\partial h}{\partial T} = \frac{h(p, T + \Delta T) - h(p, T - \Delta T)}{2\Delta T};$$

$$\frac{\partial \mu}{\partial p} = \frac{\mu(p + \Delta p, T) - \mu(p - \Delta p, T)}{2\Delta p};$$

$$\frac{\partial \mu}{\partial T} = \frac{\mu(p, T + \Delta T) - \mu(p, T - \Delta T)}{2\Delta T}.$$

Here, $\Delta p = k_p p^n$ и $\Delta T = k_T T^n$. Coefficients k_p and k_T are found in the interval 0.005–0.01.

RESULTS

The pressure and temperature before the shock are assumed to be 10^5 Pa and 288 K. The calculations are carried out for air (under normal conditions γ=1.4 and μ=0.029 kg/mol). The freestream Mach number varies from 2.5 to 15. For the case of a perfect gas, the solution to the problem exists in a tabular form.

The spectrum of flow regimes on a cone is the same as on a flat plate. However, the axisymmetric geometry of the cone leads to a change in the flow pattern. Compared to plane flows on the plate and wedge, the shock wave approaches the surface of the cone, and the thickness of the boundary layer decreases.

In a supersonic flow around a cone, in contrast to a wedge, the flow quantities are identical only on conical surfaces (and not in the entire region between the shock and the surface). When flowing around a cone, the flow in the region between the shock and the cone undergoes additional isentropic compression. At some low supersonic Mach numbers, the flow behind the shock is still supersonic, and closer to the surface of the cone it can become subsonic. Thus, a smooth transition from supersonic to subsonic speeds is observed. A subsonic zone can exist behind the shock wave, wedging into the region of supersonic flow and adjacent to the surface of the cone. At even lower supersonic speeds, the flow is no longer conical.

The distribution of flow quantities is shown in Figure 3 depending on the freestream Mach number at a fixed wedge angle θ_c=30°. While high-temperature effects have an insignificant effect on the pressure distribution, there is a significant difference in the calculation results obtained for the perfect and real gas models.

The use of the perfect gas model at high freestream Mach numbers leads to significant errors in the solution. The dependence of the relative error in calculating the temperature according to the perfect gas model and the real gas

model on the freestream Mach number is shown in Figure 4. An increase in the cone half-opening angle leads to the fact that the discrepancy between the solutions obtained by different models of the medium increases.

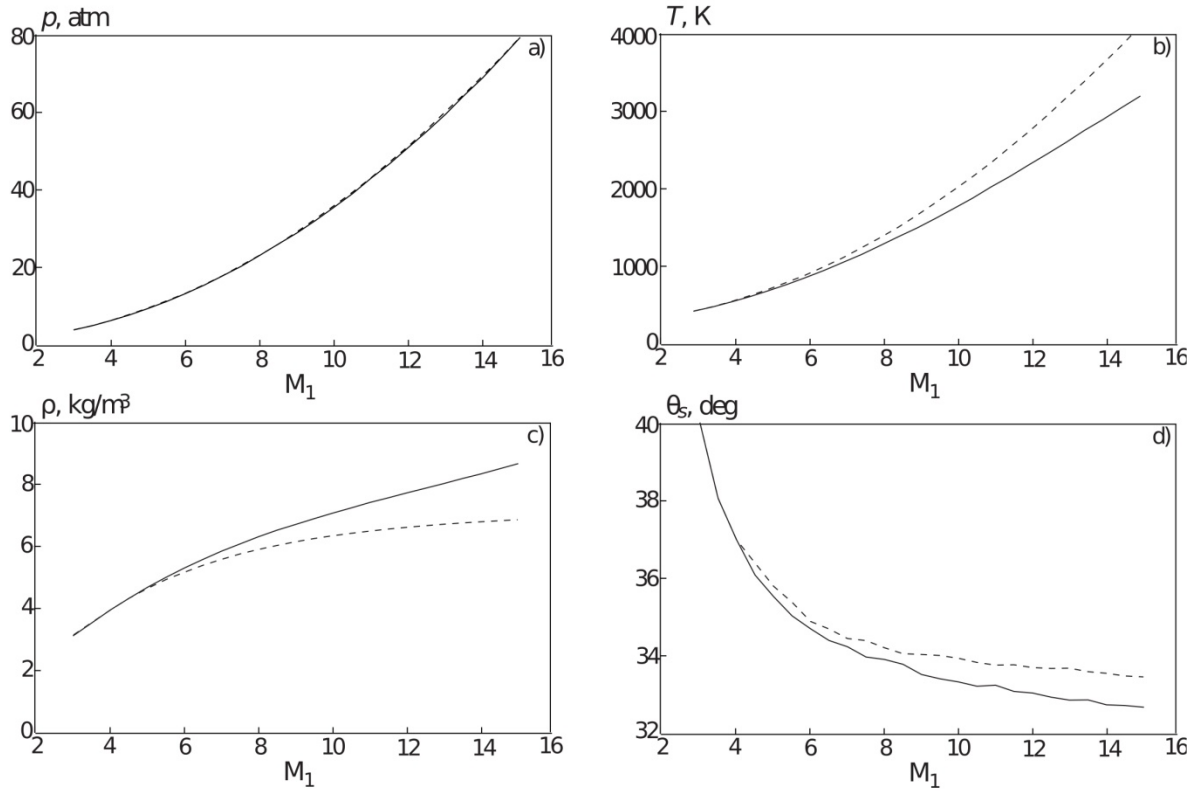

Figure 3. Distributions of pressure (a), temperature (b), density (c) and shock inclination angle (d) computed with the model of perfect gas (dashed line) and Kraiko model (solid line)

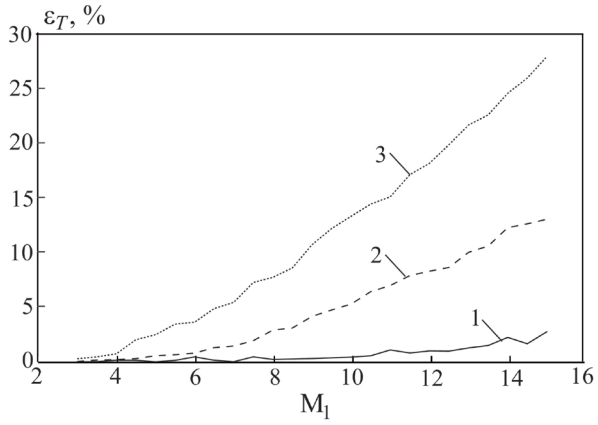

Figure 4. Relative error of temperature computed with the model of perfect gas and Kraiko model at θ_c=10° (line 1), 20° (line 2), 30° (line 3)

The difference in the angle of inclination of the shock on the wedge and the cone is shown in Figure 5 (the calculation results correspond to the perfect gas model).

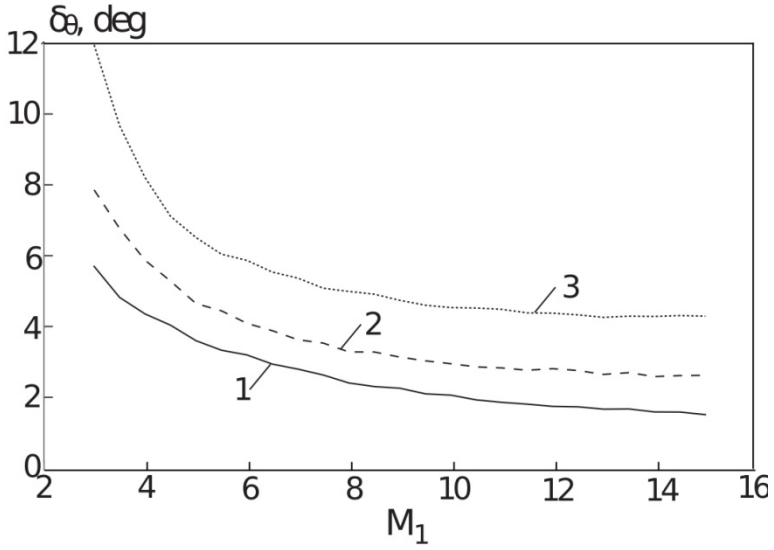

Рис. 5. Absolute error of shock inclination angle computed with the model of perfect gas at θ_c=10° (line 1), 20° (line 2), 30° (line 3)

Comparison of the results of calculations of flows formed in a supersonic flow around a wedge and a cone and obtained from the perfect and real gas models is shown in Figure 6 (at the same half-opening angles). An increase in the freestream Mach number leads to a decrease in the relative error in calculating the pressure and density. In this case, the relative error in finding the temperature in a flat and conical flow is relatively weakly dependent on the Mach number.

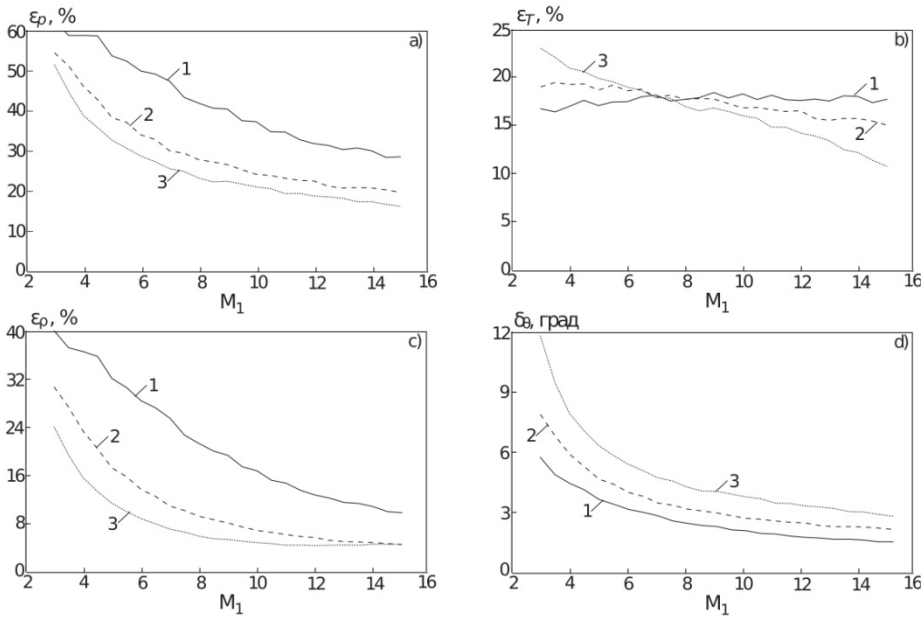

Figure 6. Relative error of pressure (a), temperature (b), density (c) and absolute error of shock inclination angle (d) at θ_c=10° (line 1), 20° (line 2), 30° (line 3)

Conclusion

A computational module has been developed to take into account the high-temperature effects that arise when a super- and hypersonic flow of an inviscid compressible gas flows around bodies. The capabilities of the developed model are shown by the example of a high-speed air flow around a sharp cone. The dependence of the distributions of the flow parameters on the cone half-opening angle and the freestream Mach number is investigated, and the results of numerical simulation obtained within the framework of the perfect and real gas model are compared.

The developed computational module allows the inclusion of promising aircraft shapes into the design systems, as well as integration with both commercial computing packages and open source software.

The study was supported by the Russian Science Foundation (project 19-71-10019).

References

1. Krasnov N.F. Aerodynamics of rotation bodies. Moscow: Publishing house «Mashinostroenie», 1964. 573 p.

2. Kraiko A.N., Tillyaeva N.I. Axisymmetric-conical and locally conical flows without swirling. Journal of Applied Mechanics and Technical Physics. 2014. Vol. 55. № 2. P. 282–298.
3. Isakova N.P., Kraiko A.N., Pyankov K.S., Tillyayeva N.I. The amplification of weak shock waves in axisymmetric supersonic flow and their reflection from an axis of symmetry. Journal of Applied Mathematics and Mechanics. 2012. Vol. 76. No. 4. P. 451–465.
4. Zubin M.A., Ostapenko N.A., Chulkov A.A. Conical gas flows with shock waves and turbulent boundary layer separation. Fluid Dynamics. 2012. Vol. 47. No. 2. P. 263–280.
5. Khabirov S.V. Swirled flows and their generalizations. Journal of Applied Mechanics and Technical Physics. 2012. Vol. 53. No. 4. P. 500–508.
6. Poplavskaya T.V., Mironov S.G. Numerical simulation of hypersonic flow around a sharp cone. Journal of Applied Mechanics and Technical Physics. 2001. Vol. 42. No. 3. P. 420–426.
7. Zheleznyakova A.L., Surzhikov S.T. Towards the creation of a virtual GLA model. Moscow: Publishing house of IPMech RAS, 2013.160 p.
8. Ding F., Liu J., Shen Ch-b., Liu Z., Chen Sh-h., Fu X. An overview of research on waverider design methodology. Acta Astronautica. 2017. Vol. 140. P. 190–205.
9. Mazhul I.I. Comparative analysis of the aerodynamics of wave-boats built on the basis of conical and plane flows. Thermophysics and Aeromechanics. 2007. Vol. 14. No. 1. P. 99–112.
10. Mazhul I.I., Rakhimov R.D. Numerical investigation of off-design regimes of flow past waveriders on the basis of axisymmetric conical flows. Fluid Dynamics. 2007. Vol. 42. No. 2. P. 302–309.
11. Blokhin A.M., Biberdorf E.A. Numerical resolution of the problem for a stationary real gas flow over a cone. Computing technology. 2015. Vol. 20. No 2. P. 29–43.

12. Biberdorf E.A., Blokhin A.M. Real gas flow about a round cone. Journal of Physics: Conference Series. 2017. Vol. 894. 012009 (8 pages).
13. Tukinakov D.A. Numerical simulation of shock-wave flows in a gas Suspension with inhomogeneous concentration of the dispersed phase. Russian Aeronautics. 2019. Vol. 62. No. 1 P. 59–65.
14. Golomazov M.M. Features of numerical simulation of a hypersonic gas flow around blunt bodies. Physico-chemical kinetics in gas dynamics. 2011. No. 2011-07-011-001.
15. Volkov K.N., Emelyanov V.N., Karpenko A.G. Numerical simulation of gas dynamic and physical-chemical processes in hypersonic flows past bodies. Numerical Methods and Programming. 2017. Vol. 18. P. 387-405.
16. Emelyanov V.N., Karpenko A.G., Volkov K.N. Simulation of hypersonic flows with equilibrium chemical reactions on graphics processor units // Acta Astronautica. 2019. Vol. 163. Part A. P. 259–271.
17. Deryugin Yu.N., Zhuchkov R.N, Zelenskiy D.K., Kozelkov A.S., Sarazov A.S., Kudimov N.F., Lipnickiy Yu.M., Panasenko A.V., Safronov A.V. Results validation multipurpose software package LOGOS at the decision of problems gasdynamics of start and flight rocets. Mathematical Modelling. 2014. Vol. 26. No. 9. P. 83–95.
18. Kozelkov A. S., Kurulin V. V., Lashkin S. V., Shagaliev R. M., and Yalozo A. V., Investigation of Supercomputer Capabilities for the Scalable Numerical Simulation of Computational Fluid Dynamics Problems in Industrial Applications // Computational Mathematics and Mathematical Physics. 2016. Vol. 56. No. 8. P. 1506–1516.
19. Kraiko A.N., Makarov V.E. Explicit analytic formulas defining the equilibrium composition and thermodynamic functions of air for temperatures from 200 to 20000 K. High Temperature. 1996. Vol. 34. № 2. P. 202–213.